Draft version October 26, 2022
Typeset using LaTeX **twocolumn** style in AASTeX631

Constrain the Merger History of Primordial-Black-Hole Binaries from GWTC-3

Lang Liu,[1,2] Zhi-Qiang You,[1,2] You Wu,[3] and Zu-Cheng Chen[1,2]

[1] *Department of Astronomy, Beijing Normal University, Beijing 100875, China*
[2] *Advanced Institute of Natural Sciences, Beijing Normal University, Zhuhai 519087, China*
[3] *College of Mathematics and Physics, Hunan University of Arts and Science, Changde, 415000, China*

ABSTRACT

Primordial black holes (PBHs), as dark matter candidates, have attracted more and more attentions as they could be possible progenitors of the heavy binary black holes (BBHs) observed by LIGO/Virgo. Accurately estimating the merger rate of PBH binaries will be crucial to reconstruct the mass distribution of PBHs. It was pointed out the merger history of PBHs may shift the merger rate distribution depending on the mass function of PBHs. In this paper, we use BBH events from LIGO/Virgo GWTC-3 data release to constrain the merger rate distribution of PBHs by taking into account the effect of merger history. It is found that the second merger process makes subdominant contribution to the total merger rate, and hence the merger history effect can be safely neglected. We also confirm that the main components of dark matter should not be made of stellar mass PBHs.

1. INTRODUCTION

The direct detection of gravitational wave (GW) from a binary black hole (BBH) coalescence Abbott et al. (2016a) has opened a new window into the universe. Over the past few years, ten BBH mergers have been reported by LIGO/Virgo during the O1 and O2 observing runs Abbott et al. (2016a,b,c, 2017a,b,c, 2018a). The progenitors of these BBHs are still unknown and under intensively investigation (see *e.g.* Bird et al. (2016); Sasaki et al. (2016); Chen & Huang (2018); Fishbach et al. (2017); Clesse & García-Bellido (2017); Antonini & Rasio (2016); Inayoshi et al. (2017); Ali-Haïmoud et al. (2017); Perna et al. (2019); Kavanagh et al. (2018); Rodriguez et al. (2015, 2016); Park et al. (2017); Belczynski et al. (2014, 2016); Woosley (2016); Rodriguez & Loeb (2018); Choksi et al. (2018); de Mink et al. (2010); de Mink & Mandel (2016)). These LIGO/Virgo BBHs present a much heavier mass distribution (in particular the source-frame primary mass of GW170729 event can be as heavy as $50.2^{+16.2}_{-10.2}M_{\odot}$ Abbott et al. (2018a)) than that inferred from X-ray observations Wiktorowicz et al. (2013); Casares & Jonker (2014); Corral-Santana et al. (2013, 2016), which would challenge the formation and evolution mechanisms of astrophysical black holes. One possible explanation for LIGO/Virgo BBHs is the primordial black holes (PBHs) Bird et al. (2016); Sasaki et al. (2016); Chen & Huang (2018) formed through the gravitational collapse of the primordial density fluctuations Hawking (1971); Carr & Hawking (1974), which may accompany the induced GWs Yuan et al. (2019a,b); Chen et al. (2019b); Yuan et al. (2019c); Cai et al. (2019a,b,c); De Luca et al. (2019); Bartolo et al. (2019b,a). On the other hand, PBHs can also be a candidate of cold dark matter (CDM), and the abundance of PBHs in CDM has been constrained by various experiments Carr et al. (2010); Barnacka et al. (2012); Graham et al. (2015); Niikura et al. (2017); Griest et al. (2013); Niikura et al. (2019); Tisserand et al. (2007); Brandt (2016); Gaggero et al. (2017); Ali-Haïmoud & Kamionkowski (2017); Aloni et al. (2017); Horowitz (2016); Chen et al. (2016); Wang et al. (2018); Abbott et al. (2018b); Magee et al. (2018); Wang et al. (2019); Chen et al. (2019a); Chen & Huang (2019); Yuan et al. (2019a); Chen et al. (2019b); Montero-Camacho et al. (2019); Laha (2019); Dasgupta et al. (2019); Gow et al. (2020).

liulang@bnu.edu.cn

zhiqiang.you@bnu.edu.cn

youwuphy@gmail.com

Corresponding author: zucheng.chen@bnu.edu.cn

In order to account for the LIGO/Virgo BBHs, the merger rate of PBH binaries has been estimated to be $17 \sim 288\ \mathrm{Gpc}^{-3}\,\mathrm{yr}^{-1}$ Chen et al. (2019a). One should notice that theoretically there exist some uncertainties in estimating the merger rate distribution of PBH binaries, and the accuracy of the estimation has been continuously improved. The merger rate of PBH binaries with monochromatic mass function has already been given in Nakamura et al. (1997); Sasaki et al. (2016) for the case where two neighboring PBHs having sufficiently small separation can form a binary in the early Universe due to the torque from the third nearest PBH. These binaries would then evolve and coalesce within the age of the Universe and finally explain the merger events observed by LIGO/Virgo Sasaki et al. (2016). Later, the merger rate estimation is improved in Ali-Haïmoud et al. (2017) by taking into account the torques exerted by all CDM (including all the PBHs and linear density perturbations), but it is also assumed that all PBHs have the same mass. It is also pointed out in Ali-Haïmoud et al. (2017) that the effects such as encountering with other PBHs, tidal field from the smooth halo, and the baryon accretion are subdominant and can be neglected when estimating the merger rate.

Various attempts have been made to estimate the merger rate distribution of PBH binaries when PBHs have an extended mass function Chen & Huang (2018); Chen et al. (2019a); Raidal et al. (2018, 2017); Liu et al. (2019a, 2020); Vaskonen & Veermäe (2019). In particular, a formalism to estimate the effect of merger history of PBHs on merger rate distribution has been developed in Liu et al. (2019b), and it is argued that the multiple-merger effect may not be ignored if PBHs have a power-law or a log-normal mass function by choosing some specific parameter values of the mass function. An accurate estimation of the merger rate will be crucial to infer the event rate of LIGO/Virgo BBHs and constrain the abundance of PBHs in CDM either through null detection of sub-solar mass PBH binaries or the null detection of stochastic GW background (SGWB) from PBH binaries.

In this paper, we will use the LVK recent released GWTC-3 data to constrain the effect of merger history on the merger rate of PBH binaries assuming all of LVK BBHs are of primordial origin. We organize the rest paper as follows. In Sec. 2, we give a brief review on calculation of merger rate of PBH binaries by accounting for the merger history effect. In Sec. 3, we describe the hierarchical Bayesian framework used to infer the PBH population parameters from GW data. In Sec. 4, we consider four commonly used PBH mass functions and present the results. Finally, we give conclusions in Sec. 5.

2. MERGER RATE DENSITY DISTRIBUTION OF PBH BINARIES

In this section, we will outline the calculation of merger rate density when taking into account the PBH merger history effect. We refer to Liu et al. (2019b) for more details.

The BBHs observed by LVK suggest that BHs should have a broad mass distribution, so we consider an extended mass function for PBHs. Here, we demand the probability distribution function of PBH mass, $P(m)$, be normalized such that

$$\int_0^\infty P(m)\,\mathrm{d}m = 1. \tag{1}$$

Assuming the fraction of PBHs in CDM is $f_{\rm pbh}$, we can estimate the abundance of PBHs in the mass interval $(m, m+\mathrm{d}m)$ as (Chen et al. 2019a)

$$0.85 f_{\rm pbh}\,P(m)\,\mathrm{d}m, \tag{2}$$

where the coefficient 0.85 is roughly the fraction of CDM in non-relativistic matter including both CDM and baryons. Following Liu et al. (2019b), we may define an average PBH mass, $m_{\rm pbh}$, as

$$\frac{1}{m_{\rm pbh}} = \int \frac{P(m)}{m}\mathrm{d}m. \tag{3}$$

Then, we can obtain the average number density of PBHs with mass m in the total number density of PBHs, $F(m)$, by (Liu et al. 2019b)

$$F(m) = P(m)\frac{m_{\rm pbh}}{m}. \tag{4}$$

We can now proceed to estimate the merger rate densities of PBH binaries by considering the merger history effect. We assume that PBHs are randomly distributed in the early Universe when they decouple from the cosmic background evolution (Nakamura et al. 1997; Sasaki et al. 2016; Ali-Haïmoud et al. 2017). Two nearest PBHs would attract each other because of the gravitational interactions. These two PBHs would obtain the angular momentum from the torque of other PBHs and form a PBH binary. The binary would emit gravitational radiations and eventually merge.

We do not intend to give a detailed derivation, but quote the results from Liu et al. (2019b) here. The merger rate density from first-merger process, $\mathcal{R}_1(t, m_i, m_j)$, is given by (Liu et al. 2019b)

$$\mathcal{R}_1(t, m_i, m_j) = \int \hat{\mathcal{R}}_1 \mathrm{d}m_l, \tag{5}$$

where

$$\hat{\mathcal{R}}_1(t, m_i, m_j, m_l) \equiv 1.32 \times 10^6 \times \left(\frac{t}{t_0}\right)^{-\frac{34}{37}} \left(\frac{f_{\rm pbh}}{m_{\rm pbh}}\right)^{\frac{53}{37}} \times m_l^{-\frac{21}{37}} (m_i m_j)^{\frac{3}{37}} (m_i + m_j)^{\frac{36}{37}} F(m_i) F(m_j) F(m_l). \tag{6}$$

Similarly, the merger rate density from second-merger process, $\mathcal{R}_2(t, m_i, m_j)$, is given by (Liu et al. 2019b)

$$\mathcal{R}_2(t, m_i, m_j) = \frac{1}{2} \int \hat{\mathcal{R}}_2(t, m_i - m_e, m_e, m_j, m_l)\ {\rm d}m_l {\rm d}m_e + \frac{1}{2} \int \hat{\mathcal{R}}_2(t, m_j - m_e, m_e, m_i, m_l)\ {\rm d}m_l {\rm d}m_e, \tag{7}$$

where

$$\hat{\mathcal{R}}_2(t, m_i, m_j, m_k, m_l) = 1.59 \times 10^4 \times \left(\frac{t}{t_0}\right)^{-\frac{31}{37}} \left(\frac{f_{\rm pbh}}{m_{\rm pbh}}\right)^{\frac{69}{37}} \times m_k^{\frac{6}{37}} m_l^{-\frac{42}{37}} (m_i + m_j)^{\frac{6}{37}} (m_i + m_j + m_k)^{\frac{72}{37}} \times F(m_i) F(m_j) F(m_k) F(m_l). \tag{8}$$

We only consider the effect of merger history up to second-merger process. Therefore the total merger rate density, $\mathcal{R}(t, m_i, m_j)$, of PBH binaries at cosmic time t with masses m_i and m_j is

$$\mathcal{R}(t, m_i, m_j) = \sum_{n=1,2} \mathcal{R}_n(t, m_i, m_j), \tag{9}$$

and the total merger rate is

$$R(t) = \int \mathcal{R}(t, m_i, m_j) {\rm d}m_i {\rm d}m_j = \sum_{n=1,2} R_n(t), \tag{10}$$

where

$$R_n(t) = \int \mathcal{R}_n(t, m_i, m_j) {\rm d}m_i {\rm d}m_j. \tag{11}$$

All the above mentioned merger rate (density) is measured at source frame. We should emphasize that although $R_2(t)$ should be smaller than $R_1(t)$ as expected, $\mathcal{R}_2(t, m_i, m_j)$ is not necessarily be smaller than $\mathcal{R}_1(t, m_i, m_j)$ (Liu et al. 2019b).

3. HIERARCHICAL BAYESIAN INFERENCE

To infer the population parameters, we adopt a hierarchical Bayesian approach by marginalizing over the uncertainty in the estimate of individual event parameters. In this section, we describe the hierarchical Bayesian inference used in the parameter estimations. The merger rate density (9) is measured in source frame, and we need to convert it into the detector frame as

$$\mathcal{R}_{\rm pop}(\theta|\Lambda) = \frac{1}{1+z} \frac{dV_{\rm c}}{dz} \mathcal{R}(\theta|\Lambda), \tag{12}$$

where z is the cosmological redshift, $\theta \equiv \{z, m_1, m_2\}$, Λ is a collection of $f_{\rm pbh}$ and the parameters from mass function $P(m)$, and $dV_{\rm c}/dz$ is the differential comoving volume. The factor $1/(1+z)$ converts time increments from the source frame to the detector frame. In this work, we take the cosmological parameters from Planck 2018 (Aghanim et al. 2020).

Given the data, $\mathbf{d} = \{d_1, d_2, \cdots, d_{N_{\rm obs}}\}$, of $N_{\rm obs}$ BBH merger events, we model the total number of events as an inhomogeneous Poisson process, yielding the likelihood (Loredo 2004; Thrane & Talbot 2018; Mandel et al. 2018)

$$\mathcal{L}(\mathbf{d}|\Lambda) \propto N_{\rm exp}^{N_{\rm obs}} e^{-N_{\rm exp}} \prod_{i=1}^{N_{\rm obs}} \frac{\int \mathcal{L}(d_i|\theta)\, \mathcal{R}_{\rm pop}(\theta|\Lambda) d\theta}{\xi(\Lambda)}, \tag{13}$$

where $N_{\rm exp} \equiv N_{\rm exp}(\Lambda)$ is the expected number of detections over the timespan of observation, and $\mathcal{L}(d_i|\theta)$ is the individual event likelihood for the ith GW event that can be derived from the individual event's posterior by reweighing with the prior on θ. Here, $\xi(\Lambda)$ quantifies selection biases for a population with parameters Λ and is defined by

$$\xi(\Lambda) = \int P_{\rm det}(\theta)\, \mathcal{R}_{\rm pop}(\theta|\Lambda)\, {\rm d}\theta, \tag{14}$$

where $P_{\rm det}(\theta)$ is the detection probability that depends on the source parameters θ. In practice, we use the simulated injections (Abbott et al. 2021a) to estimate $\xi(\Lambda)$, and Eq. (14) can be approximated by a Monte Carlo integral over found injections (Abbott et al. 2021b)

$$\xi(\Lambda) \approx \frac{1}{N_{\rm inj}} \sum_{j=1}^{N_{\rm found}} \frac{\mathcal{R}_{\rm pop}(\theta_j|\Lambda)}{p_{\rm draw}(\theta_j)}, \tag{15}$$

where $N_{\rm inj}$ is the total number of injections, $N_{\rm found}$ is the number of successfully detected injections, and $p_{\rm draw}$ is the probability density function from which the injections are drawn. Using the posterior samples from each individual event, the hyper-likelihood (13) can be estimated as

$$\mathcal{L}(\mathbf{d}|\Lambda) \propto N_{\rm exp}^{N_{\rm obs}} e^{-N_{\rm exp}} \prod_{i=1}^{N_{\rm obs}} \frac{1}{\xi(\Lambda)} \left\langle \frac{\mathcal{R}_{\rm pop}(\theta|\Lambda)}{d_L^2(z)} \right\rangle, \tag{16}$$

where $\langle \cdots \rangle$ denotes the weighted average over posterior samples of θ. The denominator $d_L^2(z)$ is the standard priors used in the LVK analysis of individual events where d_L is the luminosity distance.

Parameter	Description	Prior
$f_{\rm pbh}$	Abundance of PBH in dark matter	log-$\mathcal{U}(-4,0)$
	Lognormal PBH mass function	
$M_{\rm c}$	Central mass in $M_\odot$.	$\mathcal{U}(5,50)$
σ	Mass width.	$\mathcal{U}(0.1,2)$
	Power-law PBH mass function	
$M_{\rm min}$	Lower mass cut-off in $M_\odot$.	$\mathcal{U}(3,10)$
α	Power-law index.	$\mathcal{U}(1.05,4)$
	Broken Power-law PBH mass function	
M_*	Peak mass in $M_\odot$.	$\mathcal{U}(3,15)$
α_1	First power-law index.	$\mathcal{U}(0,15)$
α_2	Second power-law index.	$\mathcal{U}(1,3)$
	Critical collapse (CC) PBH mass function	
$M_{\rm f}$	Horizon mass scale in $M_\odot$.	$\mathcal{U}(1,50)$
α	Universal exponent.	$\mathcal{U}(0,5)$

Table 1. Parameters and their prior distributions used in the Bayesian parameter estimations. Here, $\mathcal{U}$ and log-$\mathcal{U}$ denote uniform and log-uniform distributions, respectively.

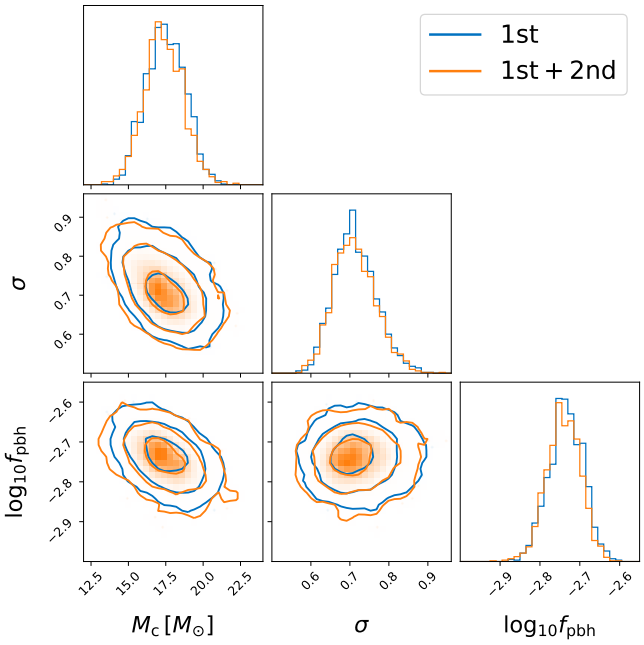

Figure 1. The marginalized one- and two-dimensional posterior distributions for hyper-parameters $\{M_c, \sigma, f_{\rm pbh}\}$ in the log-normal mass function inferred from GWTC-3. The blue color denotes the results from the first merger only, while the orange denotes the results from both the first and second mergers. The contours represent the 1σ, 2σ and 3σ credible regions, respectively.

In this work, we incorporate the PBH population distribution (9) into the `ICAROGW` (Mastrogiovanni et al. 2021) package to estimate the likelihood function (16), and use `dynesty` (Speagle 2020) sampler called from `Bilby` (Ashton et al. 2019; Romero-Shaw et al. 2020) to sample over the parameter space. We use the GW events from GWTC-3 by discarding events with false alarm rate larger than 1 yr^{-1} and events with the secondary component mass smaller than $3M_\odot$ to avoid contamination from putative events involving neutron stars following De Luca et al. (2021). A total of 69 GW events from GWTC-3 meet this criteria and the posterior samples of these BBHs are publicly available from Abbott et al. (2021c).

4. RESULTS

Based on the hierarchical statistical framework, we do the parameter estimations for four different PBH mass functions that are commonly used in the literature. These mass functions are the log-normal, power-law, broken power-law, and critical collapse (CC) distributions, respectively. We summarize the parameters and their prior distributions in Table 1. Below we show the results for each of the PBH mass function.

4.1. *Log-normal mass function*

We first consider a PBH mass function with the log-normal form (Dolgov & Silk 1993) of

$$P(m) = \frac{1}{\sqrt{2\pi}\sigma m} \exp\left(-\frac{\ln^2(m/M_c)}{2\sigma^2}\right), \tag{17}$$

where M_c represents the central mass of $mP(m)$, and σ characterizes the width of the mass spectrum. A huge class of extended mass distributions can be approximated by the log-normal mass function if PBHs are formed from a smooth symmetric peak in the inflationary power spectrum when the slow-roll approximation holds (Green 2016; Carr et al. 2017; Kannike et al. 2017). The hyper-parameters are $\Lambda = \{M_c, \sigma, f_{\rm pbh}\}$ in this case. We can then derive the averaged PBH mass and averaged number density from Eq. (3) and Eq. (4) as

$$m_{\rm pbh} = M_c \exp\left(-\frac{\sigma^2}{2}\right), \tag{18}$$

$$F(m) = \frac{M_c}{\sqrt{2\pi}\sigma m^2} \exp\left(-\frac{\sigma^2}{2} - \frac{\ln^2(m/M_c)}{2\sigma^2}\right). \tag{19}$$

Using 69 BBHs from GWTC-3 and performing the hierarchical Bayesian inference, we obtain $M_c = 17.3^{+2.2}_{-2.0} M_\odot$, $\sigma = 0.71^{+0.10}_{-0.08}$, and $f_{\rm pbh} = 1.8^{+0.3}_{-0.3} \times 10^{-3}$. In this work, we present result with median value and 90% equal-tailed credible intervals. The posteriors for the hyper-parameters $\Lambda = \{M_c, \sigma, f_{\rm pbh}\}$ are shown in Fig. 1. Note that we get a larger value of M_c than that inferred from GWTC-1 in Wu (2020) because GWTC-3

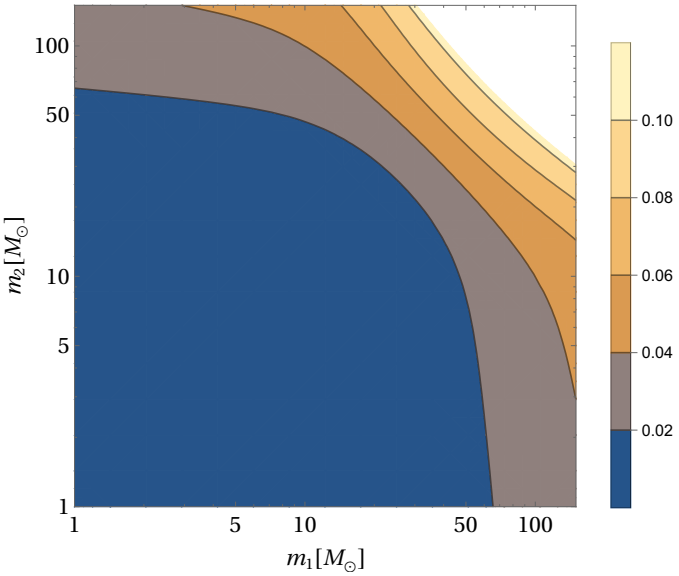

Figure 2. The ratio of merger rate density from second merger to that from first merger, $\mathcal{R}_2(t_0, m_1, m_2)/\mathcal{R}_1(t_0, m_1, m_2)$, as a function of component masses for the log-normal mass function. We have fixed the hyper-parameters $\{M_c, \sigma, f_{\rm pbh}\}$ to their best-fit values.

contains more heavier BHs than those from GWTC-1. From Eq. (10), we also infer the local merger rate as $R(t_0) = 41^{+16}_{-12}{\rm Gpc}^{-3}\,{\rm yr}^{-1}$. The results of local merger rate and abundance of PBHs are consistent with the previous estimations (Chen & Huang 2018; Chen et al. 2019a; Chen & Huang 2019; Wu 2020; Chen et al. 2022b,a), confirming that CDM cannot be dominated by the stellar-mass PBHs.

In Fig. 2, we show the ratio of merger rate density from second merger to the one from first merger, namely $\mathcal{R}_2(t_0, m_1, m_2)/\mathcal{R}_1(t_0, m_1, m_2)$, by fixing the hyper-parameters $\{M_c, \sigma, f_{\rm pbh}\}$ to their best-fit values. It can be seen that the second merger provides more contribution to the total merger rate density as component mass increases. Even though $\mathcal{R}_2(t_0, m_1, m_2)/\mathcal{R}_1(t_0, m_1, m_2)$ can reach as high as $\gtrsim$ 10%, the ratio of merger rate from second merger to that from first merger is $R_2(t_0)/R_1(t_0) = 1.0^{+0.2}_{-0.1}\%$ and is negligible. This is because the major contribution to the merger rate is from the masses less than $50M_\odot$, and the correction is negligible in this mass range. Therefore the effect of merger history can be safely ignored when estimating the merger rate of PBH binaries.

4.2. *Power-law mass function*

We next consider a PBH mass function with the power-law form (Carr 1975) of

$$P(m) = \frac{\alpha - 1}{M_{\rm min}}\left(\frac{m}{M_{\rm min}}\right)^{-\alpha}, \tag{20}$$

where $M_{\rm min}$ is the lower-mass cut-off such that $m > M_{\rm min}$, and $\alpha > 1$ is the power-law index. The power-law mass function can typically result from a broad or flat power spectrum of the curvature perturbations (De Luca et al. 2020) during radiation dominated era (Carr et al. 2016a, 2017). The hyper-parameters are $\Lambda = \{M_{\rm min}, \alpha, f_{\rm pbh}\}$ in this case. We can then derive the averaged PBH mass and averaged number density from Eq. (3) and Eq. (4) as

$$m_{\rm pbh} = M_{\rm min}\frac{\alpha}{\alpha - 1}, \tag{21}$$

$$F(m) = \frac{\alpha}{m}\left(\frac{m}{M_{\rm min}}\right)^{-\alpha}. \tag{22}$$

Using 69 BBHs from GWTC-3 and performing the hierarchical Bayesian inference, we obtain $M_{\rm min} = 6.5^{+0.3}_{-0.8}M_\odot$, $\alpha = 1.9^{+0.2}_{-0.2}$, and $f_{\rm pbh} = 2.3^{+0.3}_{-0.3}\times10^{-3}$. The posteriors for the hyper-parameters $\Lambda = \{M_{\rm min}, \alpha, f_{\rm pbh}\}$ are shown in Fig. 3. Note that we get a smaller value of α than that inferred from GWTC-1 in Wu (2020) because GWTC-3 contains more heavier BHs than those from GWTC-1. From Eq. (**??**), we also infer the local merger rate as $R_0 = 48^{+15}_{-12}{\rm Gpc}^{-3}\,{\rm yr}^{-1}$. The results of local merger rate and abundance of PBHs are consistent with the previous estimations (Chen & Huang 2018; Chen et al. 2019a; Chen & Huang 2019; Wu 2020; Chen et al. 2022b,a), confirming that CDM cannot be dominated by the stellar-mass PBHs.

In Fig. 4, we show the ratio of merger rate density from second merger to the one from first merger, namely $\mathcal{R}_2(t_0, m_1, m_2)/\mathcal{R}_1(t_0, m_1, m_2)$, by fixing the hyper-parameters $\{M_{\rm min}, \alpha, f_{\rm pbh}\}$ to their best-fit values. It can be seen that the second merger provides more contribution to the total merger rate density as component mass increases. Even though $\mathcal{R}_2(t_0, m_1, m_2)/\mathcal{R}_1(t_0, m_1, m_2)$ can reach as high as $\gtrsim$ 10%, the ratio of merger rate from second merger to that from first merger is $R_2(t_0)/R_1(t_0) = 0.9^{+0.1}_{-0.1}\%$ and is negligible. This is because the major contribution to the merger rate is from the masses less than $50M_\odot$, and the correction is negligible in this mass range. Therefore the effect of merger history can be safely ignored when estimating the merger rate of PBH binaries.

4.3. *Broken power-law mass function*

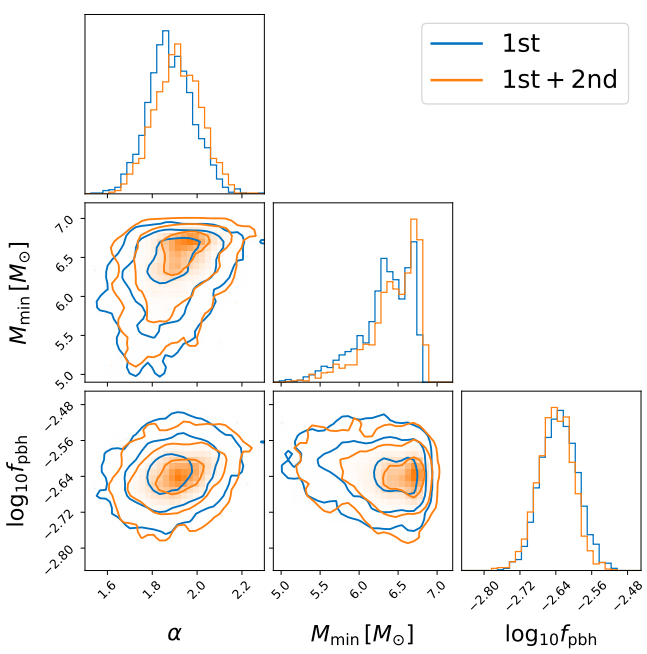

Figure 3. The marginalized one- and two-dimensional posterior distributions for hyper-parameters $\{M_{\rm min}, \alpha, f_{\rm pbh}\}$ in the power-law mass function inferred from GWTC-3. The blue color denotes the results from the first merger only, while the orange denotes the results from both the first and second mergers. The contours represent the 1σ, 2σ and 3σ credible regions, respectively.

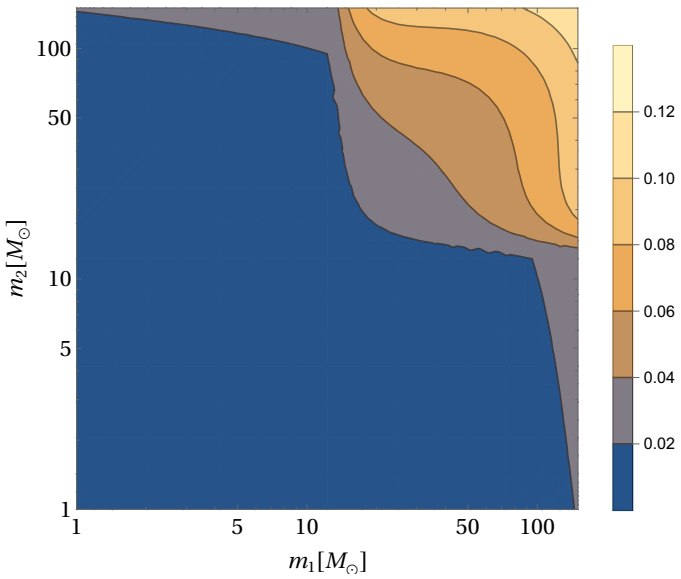

Figure 4. The ratio of merger rate density from second merger to that from first merger, $\mathcal{R}_2(t_0, m_1, m_2)/\mathcal{R}_1(t_0, m_1, m_2)$, as a function of component masses for the power-law mass function. We have fixed the hyper-parameters $\{M_{\rm min}, \alpha, f_{\rm pbh}\}$ to their best-fit values.

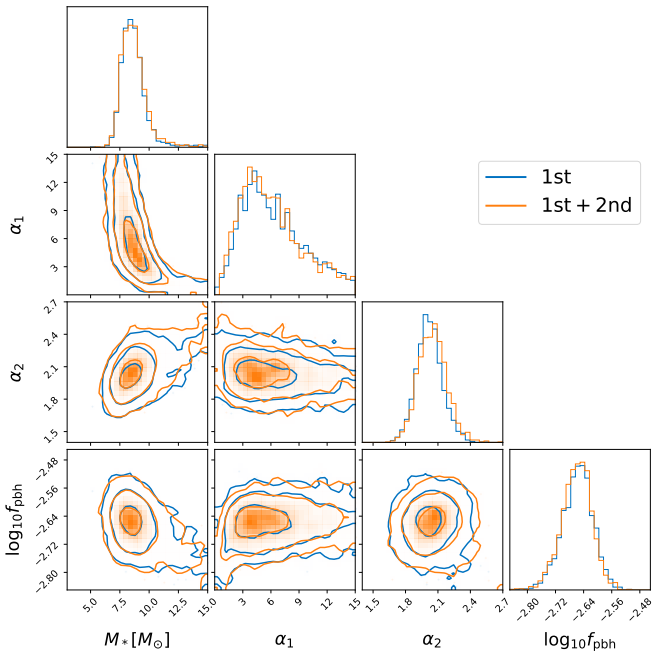

Figure 5. The marginalized one- and two-dimensional posterior distributions for hyper-parameters $\{m_*, \alpha_1, \alpha_2, f_{\rm pbh}\}$ in the broken power-law mass function inferred from GWTC-3. The blue color denotes the results from the first merger only, while the orange denotes the results from both the first and second mergers. The contours represent the 1σ, 2σ and 3σ credible regions, respectively.

We then consider a PBH mass function with the broken power-law form (Deng 2021) of

$$P(m) = \left(\frac{m_*}{\alpha_1+1} - \frac{m_*}{\alpha_2-1}\right)^{-1} \begin{cases} (\frac{m}{m_*})^{\alpha_1}, & m < m_* \\ (\frac{m}{m_*})^{-\alpha_2}, & m > m_* \end{cases}, \tag{23}$$

where m_* is the peak mass of $mP(m)$. Here $\alpha_1 > 0$ and $\alpha_2 > 1$ are two power-law indices. The broken power-law mass function is a generalization of the power-law form and can be achieved if PBHs are formed by vacuum bubbles that nucleate during inflation via quantum tunneling (Deng 2021). The hyper-parameters are $\Lambda = \{m_*, \alpha_1, \alpha_2, f_{\rm pbh}\}$ in this case. We can then derive the averaged PBH mass and averaged number density from Eq. (3) and Eq. (4) as

$$m_{\rm pbh} = \frac{\alpha_1\alpha_2}{(\alpha_1+1)(\alpha_2-1)} m_*, \tag{24}$$

$$F(m) = \frac{\alpha_1\alpha_2}{\alpha_1+\alpha_2} \begin{cases} (\frac{m}{m_*})^{\alpha_1}, & m < m_* \\ (\frac{m}{m_*})^{-\alpha_2}, & m > m_* \end{cases}. \tag{25}$$

Using 69 BBHs from GWTC-3 and performing the hierarchical Bayesian inference, we obtain $m_* =$

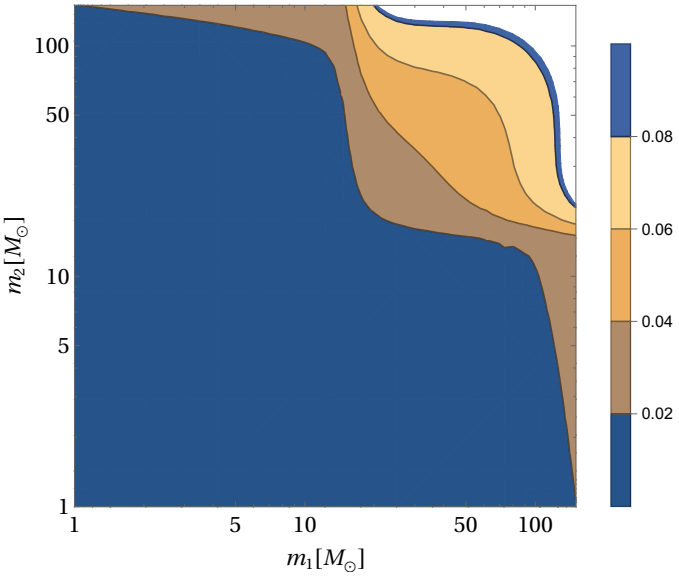

Figure 6. The ratio of merger rate density from second merger to that from first merger, $\mathcal{R}_2(t_0, m_1, m_2)/\mathcal{R}_1(t_0, m_1, m_2)$, as a function of component masses for the broken power-law mass function. We have fixed the hyper-parameters $\{m_*, \alpha_1, \alpha_2, f_{\rm pbh}\}$ to their best-fit values.

$8.6^{+2.1}_{-1.3} M_\odot$, $\alpha_1 = 5.6^{+7.1}_{-3.8}$, $\alpha_2 = 2.0^{+0.2}_{-0.2}$, and $f_{\rm pbh} = 2.2^{+0.3}_{-0.4} \times 10^{-3}$. The posteriors for the hyper-parameters $\Lambda = \{m_*, \alpha_1, \alpha_2, f_{\rm pbh}\}$ are shown in Fig. 5. From Eq. (**??**), we also infer the local merger rate as $R_0 = 46^{+15}_{-11} {\rm Gpc}^{-3}\,{\rm yr}^{-1}$. The results of local merger rate and abundance of PBHs are consistent with the previous estimations (Chen & Huang 2018; Chen et al. 2019a; Chen & Huang 2019; Wu 2020; Chen et al. 2022b,a), confirming that CDM cannot be dominated by the stellar-mass PBHs. Note that Deng (2021) obtains quite different results for the broken power-law mass function using GWTC-2 data without accounting for the uncertainties in the measurement of $\vec{\theta}$. Deng (2021) also deals with the selection effect of the GW detectors in an improper way. We emphasize that our results are more robust in the sense that we have a comprehensive treatment of the selection effect and also the measurement uncertainties. Nevertheless, our results of the broken power-law mass function are fully consistent with the results of the power-law case as expected.

In Fig. 6, we show the ratio of merger rate density from second merger to the one from first merger, namely $\mathcal{R}_2(t_0, m_1, m_2)/\mathcal{R}_1(t_0, m_1, m_2)$, by fixing the hyper-parameters $\{m_*, \alpha_1, \alpha_2, f_{\rm pbh}\}$ to their best-fit values. It can be seen that the second merger provides more contribution to the total merger rate density as component mass increases. Even though $\mathcal{R}_2(t_0, m_1, m_2)/\mathcal{R}_1(t_0, m_1, m_2)$ can reach as high as $\gtrsim$ 10%, the ratio of merger rate from second merger to that from first merger is $R_2(t_0)/R_1(t_0) = 0.9^{+0.3}_{-0.1}\%$ and is negligible. This is because the major contribution to the merger rate is from the masses less than $50 M_\odot$, and the correction is negligible in this mass range. Therefore the effect of merger history can be safely ignored when estimating the merger rate of PBH binaries.

4.4. *Critical collapse mass function*

We last consider a PBH mass function with the critical collapse form (Niemeyer & Jedamzik 1998; Yokoyama 1998; Carr et al. 2016b; Gow et al. 2022) of

$$P(m) = \frac{\alpha^2\, m^\alpha}{{M_{\rm f}}^{1+\alpha}\,\Gamma(1/\alpha)} \exp\left(-(m/M_{\rm f})^\alpha\right), \tag{26}$$

where α is a universal exponent relating to the critical collapse of radiation, and $M_{\rm f}$ is the mass scale at the order of horizon mass at the collapse epoch (Carr et al. 2016b). For this mass spectrum, there is no lower mass cut-off, but it is exponentially suppressed above the mass scale of $M_{\rm f}$. The critical collapse mass function is closely associated with a δ-function power spectrum of the density fluctuations (Niemeyer & Jedamzik 1998; Yokoyama 1998; Carr et al. 2016b; Gow et al. 2022). The hyper-parameters are $\Lambda = \{M_{\rm f}, \alpha, f_{\rm pbh}\}$ in this case. We can then derive the averaged PBH mass and averaged number density from Eq. (3) and Eq. (4) as

$$m_{\rm pbh} = \frac{M_{\rm f}\Gamma(1/\alpha)}{\alpha}, \tag{27}$$

$$F(m) = \alpha {M_{\rm f}}^{-\alpha} m^{\alpha-1} \exp\left(-(m/M_{\rm f})^\alpha\right). \tag{28}$$

Using 69 BBHs from GWTC-3 and performing the hierarchical Bayesian inference, we obtain $M_{\rm f} = 10.8^{+3.7}_{-3.6} M_\odot$, $\alpha = 1.0^{+0.2}_{-0.2}$, and $f_{\rm pbh} = 1.5^{+0.2}_{-0.2} \times 10^{-3}$. The posteriors for the hyper-parameters $\Lambda = \{M_{\rm f}, \alpha, f_{\rm pbh}\}$ are shown in Fig. 7. From Eq. (**??**), we also infer the local merger rate as $R_0 = 49^{+26}_{-16} {\rm Gpc}^{-3}\,{\rm yr}^{-1}$. The results of local merger rate and abundance of PBHs are consistent with the previous estimations (Chen & Huang 2018; Chen et al. 2019a; Chen & Huang 2019; Wu 2020; Chen et al. 2022b,a), confirming that CDM cannot be dominated by the stellar-mass PBHs.

In Fig. 8, we show the ratio of merger rate density from second merger to the one from first merger, namely $\mathcal{R}_2(t_0, m_1, m_2)/\mathcal{R}_1(t_0, m_1, m_2)$, by fixing the hyper-parameters $\{M_{\rm f}, \alpha, f_{\rm pbh}\}$ to their best-fit values. It can be seen that the second merger provides more contribution to the total merger rate density as component mass increases. Even though $\mathcal{R}_2(t_0, m_1, m_2)/\mathcal{R}_1(t_0, m_1, m_2)$ can reach as high as $\gtrsim$ 10%, the ratio of merger

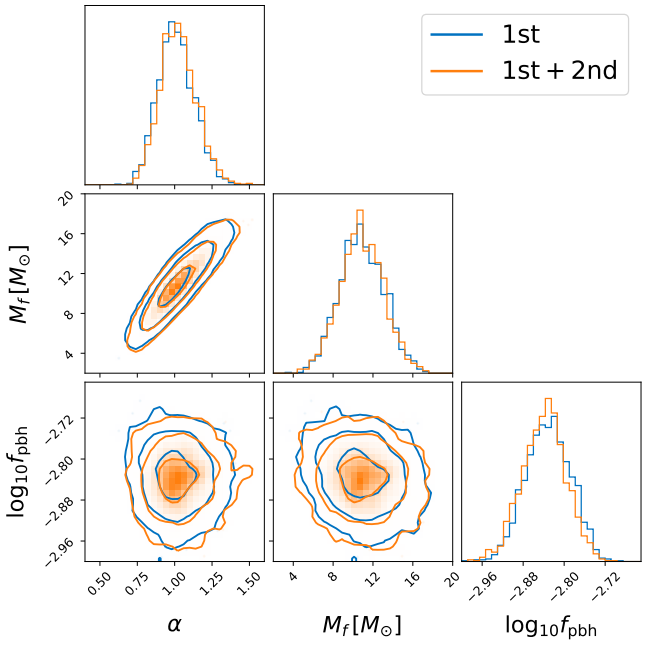

Figure 7. The marginalized one- and two-dimensional posterior distributions for hyper-parameters $\{M_{\rm f}, \alpha, f_{\rm pbh}\}$ in the critical collapse mass function inferred from GWTC-3. The blue color denotes the results from the first merger only, while the orange denotes the results from both the first and second mergers. The contours represent the 1σ, 2σ and 3σ credible regions, respectively.

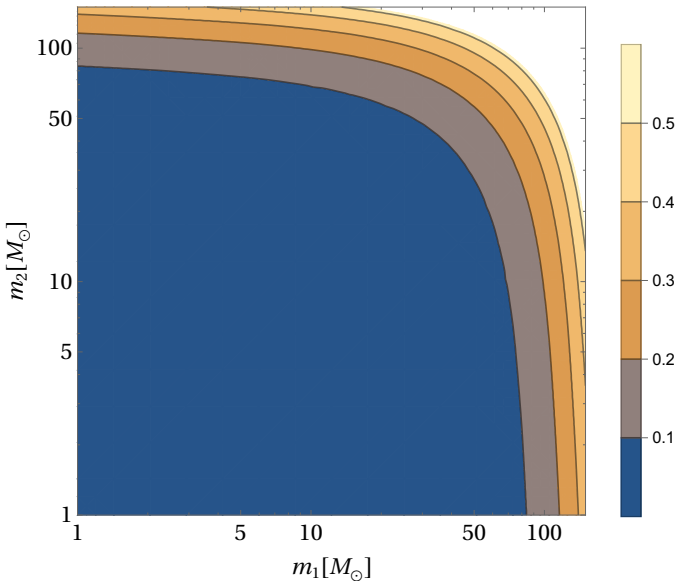

Figure 8. The ratio of merger rate density from second merger to that from first merger, $\mathcal{R}_2(t_0, m_1, m_2)/\mathcal{R}_1(t_0, m_1, m_2)$, as a function of component masses for the critical collapse mass function. We have fixed the hyper-parameters $\{M_{\rm f}, \alpha, f_{\rm pbh}\}$ to their best-fit values.

rate from second merger to that from first merger is $R_2(t_0)/R_1(t_0) = 2.2^{+1.3}_{-0.1}\%$ and is negligible. This is because the major contribution to the merger rate is from the masses less than $50M_\odot$, and the correction is negligible in this mass range. Therefore the effect of merger history can be safely ignored when estimating the merger rate of PBH binaries.

5. CONCLUSION

In this work, we use 69 BBHs from GWTC-3 to constrain the merger history of PBH binaries by assuming the observed BBHs from LVK are attributed to PBHs. We perform comprehensive Bayesian analyses by considering four commonly used PBH mass functions in literature, namely the log-normal, power-law, broken power-law, and critical collapse mass functions.

We summarize the key results in Table 2. It can be seen that the contribution of merger rate from second merger to the total merger rate is less than 5%. Therefore, the merger history of PBH binaries has subdominant effect, and this effect can be neglected when evaluating the merger rate of PBH binaries. It can also be seen that the Bayes factors for the model with second merger vesus the model with only the first merger, $\mathrm{BF}^{\rm 2nd}_{\rm 1st}$, are all smaller than 3, indicating the evidence for the second merger is "not worth more than a bare mention" (Kass & Raftery 1995). In this sense, the Bayes factors also imply the effect of merger history can be ignored.

Furthermore, for all the four mass functions, we infer the abundance of PBH in cold dark matter, $f_{\rm pbh}$, to be at the order of $\mathcal{O}(10^{-3})$. The results of local merger rate and abundance of PBHs are consistent with the previous estimations (Chen & Huang 2018; Chen et al. 2019a; Chen & Huang 2019; Wu 2020; Chen et al. 2022b,a), confirming that CDM cannot be dominated by the stellar-mass PBHs.

We also compute the Bayes factors between the models with different PBH mass functions. The Bayes factors $\mathrm{BF}_{\rm PL}$ are estimated by taking the model with power-law mass function as the fiducial model. We find that $\mathrm{BF}^{\rm LG}_{\rm PL}$ has the largest value, indicating that GWTC-3 can be best fitted by the log-normal mass function among the four mass functions considered in this work. Our findings contradict with the results from Deng (2021) claiming that broken power-law mass function can fit better than the log-normal form. There are some drawbacks from analyses in Deng (2021). Firstly, Deng (2021) neglects the uncertainties in the measurement of each event's masses and completely ignores redshift evolution of the merger rate. Secondly, Deng (2021) deals with the selection effect of GW detectors

	LN	PL	BPL	CC
$\mathrm{BF}^{\mathrm{2nd}}_{\mathrm{1st}}$	0.9	0.4	0.69	1.2
$\mathrm{BF}_{\mathrm{PL}}$	166	1	2	139
$10^3 f_{\mathrm{pbh}}$	$1.8^{+0.3}_{-0.3}$	$2.3^{+0.3}_{-0.3}$	$2.2^{+0.3}_{-0.4}$	$1.5^{+0.2}_{-0.2}$
$10^2 R_2/R_1$	$1.0^{+0.2}_{-0.1}$	$0.9^{+0.1}_{-0.1}$	$0.9^{+0.3}_{-0.1}$	$2.2^{+1.3}_{-0.5}$

Table 2. Summary of the key results for the log-normal (LN), power-law (PL), broken power-law (BPL), and critical collapse (CC) mass functions. The first row, $\mathrm{BF}^{\mathrm{2nd}}_{\mathrm{1st}}$, shows the Bayes factors for the model with 2nd merger versus the model with only 1st merger; the second row, $\mathrm{BF}_{\mathrm{PL}}$, shows the Bayes factors for the model with different PBH mass function versus the model with the power-law PBH mass function by accounting for the second merger effect; the third row, f_{pbh}, shows the abundance of PBH in dark matter inferred from different models by accounting for the second merger effect; the last row, R_2/R_1, shows the merger rate ratio between the second merger and the first merger.

in an improper way. In this sense, we disagree with Deng (2021) and conclude that the most frequently used log-normal mass function can fit GWTC-3 best among the four mass functions.

We would also like to thank Xingjiang Zhu, Xiao-Jin Liu, Shen-Shi Du, and Zhu Yi for useful discussions. Z.-C.C. is supported by the China Postdoctoral Science Foundation Fellowship No. 2022M710429. This research has made use of data, software and/or web tools obtained from the Gravitational Wave Open Science Center (https://www.gw-openscience.org/), a service of LIGO Laboratory, the LIGO Scientific Collaboration, the Virgo Collaboration, and the KAGRA Collaboration. LIGO Laboratory and Advanced LIGO are funded by the United States National Science Foundation (NSF) as well as the Science and Technology Facilities Council (STFC) of the United Kingdom, the Max-Planck-Society (MPS), and the State of Niedersachsen/Germany for support of the construction of Advanced LIGO and construction and operation of the GEO600 detector. Additional support for Advanced LIGO was provided by the Australian Research Council. Virgo is funded, through the European Gravitational Observatory (EGO), by the French Centre National de Recherche Scientifique (CNRS), the Italian Istituto Nazionale di Fisica Nucleare (INFN) and the Dutch Nikhef, with contributions by institutions from Belgium, Germany, Greece, Hungary, Ireland, Japan, Monaco, Poland, Portugal, Spain. The construction and operation of KAGRA are funded by Ministry of Education, Culture, Sports, Science and Technology (MEXT), and Japan Society for the Promotion of Science (JSPS), National Research Foundation (NRF) and Ministry of Science and ICT (MSIT) in Korea, Academia Sinica (AS) and the Ministry of Science and Technology (MoST) in Taiwan.

REFERENCES

Abbott, B. P., et al. 2016a, Phys. Rev. Lett., 116, 061102, doi: 10.1103/PhysRevLett.116.061102

—. 2016b, Phys. Rev. Lett., 116, 241103, doi: 10.1103/PhysRevLett.116.241103

—. 2016c, Phys. Rev., X6, 041015, doi: 10.1103/PhysRevX.6.041015

—. 2017a, Phys. Rev. Lett., 118, 221101, doi: 10.1103/PhysRevLett.118.221101

—. 2017b, Astrophys. J., 851, L35, doi: 10.3847/2041-8213/aa9f0c

—. 2017c, Phys. Rev. Lett., 119, 141101, doi: 10.1103/PhysRevLett.119.141101

—. 2018a. https://arxiv.org/abs/1811.12907

—. 2018b, Phys. Rev. Lett., 121, 231103, doi: 10.1103/PhysRevLett.121.231103

Abbott, R., et al. 2021a, doi: https://doi.org/10.5281/zenodo.5546676

—. 2021b. https://arxiv.org/abs/2111.03634

—. 2021c, The population of merging compact binaries inferred using gravitational waves through GWTC-3 - Data release, v1, Zenodo, doi: 10.5281/zenodo.5655785

Aghanim, N., et al. 2020, Astron. Astrophys., 641, A6, doi: 10.1051/0004-6361/201833910

Ali-Haïmoud, Y., & Kamionkowski, M. 2017, Phys. Rev., D95, 043534, doi: 10.1103/PhysRevD.95.043534

Ali-Haïmoud, Y., Kovetz, E. D., & Kamionkowski, M. 2017, Phys. Rev., D96, 123523, doi: 10.1103/PhysRevD.96.123523

Aloni, D., Blum, K., & Flauger, R. 2017, JCAP, 1705, 017, doi: 10.1088/1475-7516/2017/05/017

Antonini, F., & Rasio, F. A. 2016, Astrophys. J., 831, 187, doi: 10.3847/0004-637X/831/2/187
Ashton, G., et al. 2019, Astrophys. J. Suppl., 241, 27, doi: 10.3847/1538-4365/ab06fc
Barnacka, A., Glicenstein, J. F., & Moderski, R. 2012, Phys. Rev., D86, 043001, doi: 10.1103/PhysRevD.86.043001
Bartolo, N., De Luca, V., Franciolini, G., et al. 2019a, Phys. Rev. Lett., 122, 211301, doi: 10.1103/PhysRevLett.122.211301
—. 2019b, Phys. Rev., D99, 103521, doi: 10.1103/PhysRevD.99.103521
Belczynski, K., Buonanno, A., Cantiello, M., et al. 2014, Astrophys. J., 789, 120, doi: 10.1088/0004-637X/789/2/120
Belczynski, K., Holz, D. E., Bulik, T., & O'Shaughnessy, R. 2016, Nature, 534, 512, doi: 10.1038/nature18322
Bird, S., Cholis, I., Muñoz, J. B., et al. 2016, Phys. Rev. Lett., 116, 201301, doi: 10.1103/PhysRevLett.116.201301
Brandt, T. D. 2016, Astrophys. J., 824, L31, doi: 10.3847/2041-8205/824/2/L31
Cai, R.-G., Guo, Z.-K., Liu, J., Liu, L., & Yang, X.-Y. 2019a. https://arxiv.org/abs/1912.10437
Cai, R.-g., Pi, S., & Sasaki, M. 2019b, Phys. Rev. Lett., 122, 201101, doi: 10.1103/PhysRevLett.122.201101
Cai, R.-G., Pi, S., Wang, S.-J., & Yang, X.-Y. 2019c, doi: 10.1088/1475-7516/2019/10/059
Carr, B., Kuhnel, F., & Sandstad, M. 2016a, Phys. Rev., D94, 083504, doi: 10.1103/PhysRevD.94.083504
Carr, B., Raidal, M., Tenkanen, T., Vaskonen, V., & Veermäe, H. 2017, Phys. Rev., D96, 023514, doi: 10.1103/PhysRevD.96.023514
Carr, B. J. 1975, Astrophys. J., 201, 1, doi: 10.1086/153853
Carr, B. J., & Hawking, S. W. 1974, Mon. Not. Roy. Astron. Soc., 168, 399
Carr, B. J., Kohri, K., Sendouda, Y., & Yokoyama, J. 2010, Phys. Rev., D81, 104019, doi: 10.1103/PhysRevD.81.104019
—. 2016b, Phys. Rev. D, 94, 044029, doi: 10.1103/PhysRevD.94.044029
Casares, J., & Jonker, P. G. 2014, Space Sci. Rev., 183, 223, doi: 10.1007/s11214-013-0030-6
Chen, L., Huang, Q.-G., & Wang, K. 2016, JCAP, 1612, 044, doi: 10.1088/1475-7516/2016/12/044
Chen, Z.-C., Du, S.-S., Huang, Q.-G., & You, Z.-Q. 2022a. https://arxiv.org/abs/2205.11278
Chen, Z.-C., Huang, F., & Huang, Q.-G. 2019a, Astrophys. J., 871, 97, doi: 10.3847/1538-4357/aaf581
Chen, Z.-C., & Huang, Q.-G. 2018, Astrophys. J., 864, 61, doi: 10.3847/1538-4357/aad6e2
—. 2019. https://arxiv.org/abs/1904.02396
Chen, Z.-C., Yuan, C., & Huang, Q.-G. 2019b. https://arxiv.org/abs/1910.12239
—. 2022b, Phys. Lett. B, 829, 137040, doi: 10.1016/j.physletb.2022.137040
Choksi, N., Volonteri, M., Colpi, M., Gnedin, O. Y., & Li, H. 2018. https://arxiv.org/abs/1809.01164
Clesse, S., & García-Bellido, J. 2017, Phys. Dark Univ., 15, 142, doi: 10.1016/j.dark.2016.10.002
Corral-Santana, J. M., Casares, J., Munoz-Darias, T., et al. 2016, Astron. Astrophys., 587, A61, doi: 10.1051/0004-6361/201527130
Corral-Santana, J. M., Casares, J., Muñoz-Darias, T., et al. 2013, Science, 339, 1048, doi: 10.1126/science.1228222
Dasgupta, B., Laha, R., & Ray, A. 2019. https://arxiv.org/abs/1912.01014
De Luca, V., Franciolini, G., Kehagias, A., & Riotto, A. 2019. https://arxiv.org/abs/1911.09689
De Luca, V., Franciolini, G., Pani, P., & Riotto, A. 2021, JCAP, 05, 003, doi: 10.1088/1475-7516/2021/05/003
De Luca, V., Franciolini, G., & Riotto, A. 2020, Phys. Lett. B, 807, 135550, doi: 10.1016/j.physletb.2020.135550
de Mink, S. E., Cantiello, M., Langer, N., & Pols, O. R. 2010, in American Institute of Physics Conference Series, Vol. 1314, American Institute of Physics Conference Series, ed. V. Kalogera & M. van der Sluys, 291–296, doi: 10.1063/1.3536387
de Mink, S. E., & Mandel, I. 2016, Mon. Not. Roy. Astron. Soc., 460, 3545, doi: 10.1093/mnras/stw1219
Deng, H. 2021, JCAP, 04, 058, doi: 10.1088/1475-7516/2021/04/058
Dolgov, A., & Silk, J. 1993, Phys. Rev., D47, 4244, doi: 10.1103/PhysRevD.47.4244
Fishbach, M., Holz, D. E., & Farr, B. 2017, Astrophys. J., 840, L24, doi: 10.3847/2041-8213/aa7045
Gaggero, D., Bertone, G., Calore, F., et al. 2017, Phys. Rev. Lett., 118, 241101, doi: 10.1103/PhysRevLett.118.241101
Gow, A. D., Byrnes, C. T., & Hall, A. 2022, Phys. Rev. D, 105, 023503, doi: 10.1103/PhysRevD.105.023503
Gow, A. D., Byrnes, C. T., Hall, A., & Peacock, J. A. 2020, JCAP, 2001, 031, doi: 10.1088/1475-7516/2020/01/031
Graham, P. W., Rajendran, S., & Varela, J. 2015, Phys. Rev., D92, 063007, doi: 10.1103/PhysRevD.92.063007
Green, A. M. 2016, Phys. Rev., D94, 063530, doi: 10.1103/PhysRevD.94.063530
Griest, K., Cieplak, A. M., & Lehner, M. J. 2013, Phys. Rev. Lett., 111, 181302, doi: 10.1103/PhysRevLett.111.181302
Hawking, S. 1971, Mon. Not. Roy. Astron. Soc., 152, 75
Horowitz, B. 2016. https://arxiv.org/abs/1612.07264

Inayoshi, K., Hirai, R., Kinugawa, T., & Hotokezaka, K. 2017, Mon. Not. Roy. Astron. Soc., 468, 5020, doi: 10.1093/mnras/stx757

Kannike, K., Marzola, L., Raidal, M., & Veermäe, H. 2017, JCAP, 1709, 020, doi: 10.1088/1475-7516/2017/09/020

Kass, R. E., & Raftery, A. E. 1995, Journal of the American Statistical Association, 90, 773, doi: 10.1080/01621459.1995.10476572

Kavanagh, B. J., Gaggero, D., & Bertone, G. 2018, Phys. Rev., D98, 023536, doi: 10.1103/PhysRevD.98.023536

Laha, R. 2019, Phys. Rev. Lett., 123, 251101, doi: 10.1103/PhysRevLett.123.251101

Liu, L., Guo, Z.-K., & Cai, R.-G. 2019a, Phys. Rev., D99, 063523, doi: 10.1103/PhysRevD.99.063523

—. 2019b, Eur. Phys. J., C79, 717, doi: 10.1140/epjc/s10052-019-7227-0

Liu, L., Guo, Z.-K., Cai, R.-G., & Kim, S. P. 2020. https://arxiv.org/abs/2001.02984

Loredo, T. J. 2004, AIP Conf. Proc., 735, 195, doi: 10.1063/1.1835214

Magee, R., Deutsch, A.-S., McClincy, P., et al. 2018, Phys. Rev., D98, 103024, doi: 10.1103/PhysRevD.98.103024

Mandel, I., Farr, W. M., & Gair, J. R. 2018. https://arxiv.org/abs/1809.02063

Mastrogiovanni, S., Leyde, K., Karathanasis, C., et al. 2021, Phys. Rev. D, 104, 062009, doi: 10.1103/PhysRevD.104.062009

Montero-Camacho, P., Fang, X., Vasquez, G., Silva, M., & Hirata, C. M. 2019, JCAP, 1908, 031, doi: 10.1088/1475-7516/2019/08/031

Nakamura, T., Sasaki, M., Tanaka, T., & Thorne, K. S. 1997, Astrophys. J., 487, L139, doi: 10.1086/310886

Niemeyer, J. C., & Jedamzik, K. 1998, Phys. Rev. Lett., 80, 5481, doi: 10.1103/PhysRevLett.80.5481

Niikura, H., Takada, M., Yokoyama, S., Sumi, T., & Masaki, S. 2019. https://arxiv.org/abs/1901.07120

Niikura, H., et al. 2017. https://arxiv.org/abs/1701.02151

Park, D., Kim, C., Lee, H. M., Bae, Y.-B., & Belczynski, K. 2017, Mon. Not. Roy. Astron. Soc., 469, 4665, doi: 10.1093/mnras/stx1015

Perna, R., Wang, Y.-H., Leigh, N., & Cantiello, M. 2019. https://arxiv.org/abs/1901.03345

Raidal, M., Spethmann, C., Vaskonen, V., & Veermäe, H. 2018. https://arxiv.org/abs/1812.01930

Raidal, M., Vaskonen, V., & Veermäe, H. 2017, JCAP, 1709, 037, doi: 10.1088/1475-7516/2017/09/037

Rodriguez, C. L., Chatterjee, S., & Rasio, F. A. 2016, Phys. Rev., D93, 084029, doi: 10.1103/PhysRevD.93.084029

Rodriguez, C. L., & Loeb, A. 2018, Astrophys. J., 866, L5, doi: 10.3847/2041-8213/aae377

Rodriguez, C. L., Morscher, M., Pattabiraman, B., et al. 2015, Phys. Rev. Lett., 115, 051101, doi: 10.1103/PhysRevLett.116.029901,10.1103/PhysRevLett.115.051101

Romero-Shaw, I. M., et al. 2020, Mon. Not. Roy. Astron. Soc., 499, 3295, doi: 10.1093/mnras/staa2850

Sasaki, M., Suyama, T., Tanaka, T., & Yokoyama, S. 2016, Phys. Rev. Lett., 117, 061101, doi: 10.1103/PhysRevLett.117.061101

Speagle, J. S. 2020, Mon. Not. Roy. Astron. Soc., 493, 3132, doi: 10.1093/mnras/staa278

Thrane, E., & Talbot, C. 2018. https://arxiv.org/abs/1809.02293

Tisserand, P., et al. 2007, Astron. Astrophys., 469, 387, doi: 10.1051/0004-6361:20066017

Vaskonen, V., & Veermäe, H. 2019. https://arxiv.org/abs/1908.09752

Wang, S., Terada, T., & Kohri, K. 2019. https://arxiv.org/abs/1903.05924

Wang, S., Wang, Y.-F., Huang, Q.-G., & Li, T. G. F. 2018, Phys. Rev. Lett., 120, 191102, doi: 10.1103/PhysRevLett.120.191102

Wiktorowicz, G., Belczynski, K., & Maccarone, T. J. 2013. https://arxiv.org/abs/1312.5924

Woosley, S. E. 2016, Astrophys. J., 824, L10, doi: 10.3847/2041-8205/824/1/L10

Wu, Y. 2020, Phys. Rev. D, 101, 083008, doi: 10.1103/PhysRevD.101.083008

Yokoyama, J. 1998, Phys. Rev. D, 58, 107502, doi: 10.1103/PhysRevD.58.107502

Yuan, C., Chen, Z.-C., & Huang, Q.-G. 2019a, Phys. Rev., D100, 081301, doi: 10.1103/PhysRevD.100.081301

—. 2019b. https://arxiv.org/abs/1910.09099

—. 2019c. https://arxiv.org/abs/1912.00885